

Spin Lifetime Measurements in a 14nm GaAs Quantum Well

David Meyer

A senior thesis submitted to the faculty of
Brigham Young University
in partial fulfillment of the requirements for the degree of

Bachelor of Science

John Colton, Advisor

Department of Physics and Astronomy

Brigham Young University

August 2012

Copyright © 2012 David Meyer

All Rights Reserved

ABSTRACT

Spin Lifetime Measurements in a 14nm GaAs Quantum Well

David Meyer

Department of Physics and Astronomy

Bachelor of Science

We have measured T_1 spin lifetimes of a 14 nm modulation-doped (100) GaAs quantum well using a time-resolved pump-probe Kerr rotation technique. T_1 lifetimes in excess of 1 microsecond were measured at 1.5 K and 5.5 T. We observed effects from nuclear polarization, which could be removed by simultaneous nuclear magnetic resonance, along with two distinct lifetimes under some conditions that likely result from probing two distinct subsets of electrons. Finally, we found certain conditions that would produce different cw Kerr rotation responses depending upon the sweep direction of the probe laser wavelength.

Keywords: spintronics, electron spin, spin flip lifetime, gallium arsenide, quantum well, trion

Contents

Table of Contents	v
List of Figures	vii
1 Introduction	1
1.1 Background	2
1.1.1 Electron Spin & Spin Lifetimes	2
1.1.2 Semiconductors & Heterostructures	3
1.1.3 Relevant Particles & Quasi-Particles	5
2 Long-lived Electron Spins in a Modulation Doped (100) GaAs Quantum Well	9
Introduction	11
Sample	12
Spin Polarization and Detection	12
Experimental Setup	13
Results	14
Discussion	15
Conclusion	16
Bibliography	17
3 Further Discussion	17
3.1 An Unexplained Effect	17
3.2 Conclusion	19
Bibliography	21
Index	23

List of Figures

1.1	Schematic of GaAs/AlGaAs Quantum Well	4
1.2	Approximate band structure of GaAs near $\vec{k} = 0$	6
2.1	Heavy and Light Hole Trion Transitions and Selection Rules	12
2.2	Representative cw Kerr Rotation Signal Scan	13
2.3	Summary of cw Kerr Rotation Scans and Trion Peak Positions	13
2.4	Representative Spin Decays	14
2.5	Summary of Electron Spin Lifetimes	14
2.6	Spin Decay with and without Nuclear Polarization	15
2.7	Spin Lifetimes as a Function of Probe Laser Wavelength	16
3.1	Wavelength Dependent cw Kerr Rotation Scans and Pump Beam Blocking Times.	18

Chapter 1

Introduction

In recent years, the field of spintronics has seen significant attention. The possibility to apply not just the electrons themselves, but their spin, to the creation of new, spin-based electronics holds great potential for increases in both capacity and speed. Electronic spin states (“spins”) are particularly suitable for use as bits in a quantum computer. [1] For these applications to become a reality, it is necessary to obtain a deeper understanding of how to manipulate spins and how they interact with their environment. Ultimately, the material that contains the electrons becomes the most important factor in the study of spin dynamics since spins are heavily affected by the material’s structure. With the discovery of long spin lifetimes in gallium arsenide (GaAs) [2], an optically accessible substance with transitions that match readily-available Ti:sapphire lasers, various structures of GaAs have been tested for favorable spin dynamic properties. One such structure that has shown promise in the past is a 14nm GaAs/AlGaAs quantum well. [3] The spin dynamics of this sample are the focus of the present study.

This paper is organized into three chapters. Chapter 1 includes background information detailing terminology and concepts related to electron spin lifetimes. Chapter 2 is the journal article submitted for publication in the Journal of Applied Physics. It is this article that presents the experimental methods and the bulk of our results. Finally, Chapter 3 discusses results not included

in the submitted paper.

1.1 Background

1.1.1 Electron Spin & Spin Lifetimes

Spin is an intrinsic property of all elementary particles and is used in reference to the spin angular momentum of the particle. Unlike orbital angular momentum, which is the other contribution to the total angular momentum of a particle, spin does not have a strict classical analog. It is, however, similar to classical spin ($S = I \cdot \omega$) in that it does not depend on the position of the particle. Unlike classical spin, the magnitude of the spin for a given type of particle is always constant, being determined by the quantized properties of the particle. The lone, variable parameter is the direction of the spin. In the case of electrons, the spin can be measured to be either $+1/2$ or $-1/2$, representing either aligned or anti-aligned to the measurement axis. Since any given measurement of an electron's spin can only return one of two possibilities, electron spin could be used in a binary system such as a bit in a quantum computer. Furthermore, electron spins interact with electromagnetic waves and magnetic fields as if they were ideal magnetic dipoles, allowing for simple control of such a bit. Of course, attempting to manipulate the spin of a single electron is usually impractical, so it is common to work with a group of electrons to form a spin population. The degree to which the spins of a population are aligned is known as the spin polarization. Therefore, it is the spin polarization that is measured when determining the electron spin lifetime.

The term “spin lifetime” can refer to one of three lifetimes that characterize the electron spin dynamics of a sample: T_1 , T_2 , and T_2^* . Of these, T_2 is the most relevant for quantum computation as it measures how long a spin population will stay spin polarized while operations are performed.

T_1 , known as the spin-flip time, is the time it takes for the spin to flip from $+1/2$ to $-1/2$ or vice-versa. This measurement is typically accomplished by using a magnetic field to align the spins in

one direction, then flipping the spins to be anti-aligned to the magnetic field. The spin polarization is then monitored as the spins naturally decay back to their equilibrium state. Since the spins are aligned parallel to the magnetic field, this setup is said to be in longitudinal or Faraday geometry. Of the three lifetimes, this is typically the longest and is generally considered to be the upper bound for T_2 .

T_2 , known as the dephasing time, is the time it takes for an aligned spin polarized population to dephase. Since data encoded via spin polarized electrons would need to persist for at least the duration of one computation, this time is the determining factor for a sample's viable use in a quantum computer. T_2 (and the related T_2^*) is measured with the spins aligned perpendicular to the magnetic field in what is known as a transverse or Voigt geometry. Unfortunately, this time is the most difficult to measure.

T_2^* , known as the inhomogeneous dephasing time, measures the effect of sample inhomogeneities on the dephasing of the spin population. An inhomogeneous sample can cause spins to behave differently for different locations within the same sample. These differences then result in a general dephasing of the spin polarization that is cumulative with the natural dephasing (T_2) of the spins. T_2^* is the shortest of the three lifetimes and is considered to be the lower bound of T_2 .

1.1.2 Semiconductors & Heterostructures

Semiconductors are commonly used as the source of electrons for spin populations since their band structure allows one to separate out a smaller portion of electrons through excitation to the conduction band. The spins of this smaller, isolated population are then less likely to interact with their surroundings, limiting unwanted dephasing of the spin population. It is further possible to fine tune the number of electrons available for a spin population in a semiconductor through a process called doping. Doping a semiconductor involves replacing atoms from the semiconductor's structure with atoms from a neighboring column in the periodic table. This leaves the overall

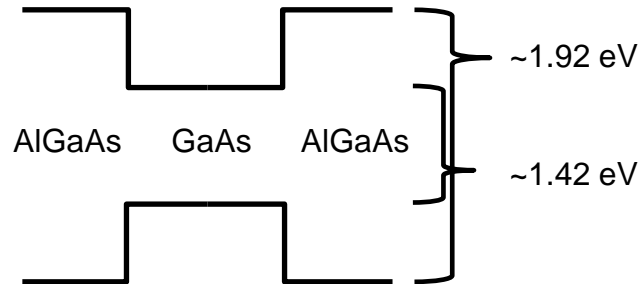


Figure 1.1 Schematic of GaAs/AlGaAs Quantum Well. Placing materials with lower band gap energies between materials of higher band gap energies creates a potential well that constrains the free electrons. If the layers in the above schematic are imagined as planes perpendicular to the page, a quantum well is formed.

structure with either too many or too few electrons which corresponds to a change in the number of free electrons in the conduction band. Taking GaAs as an example, an n -type dopant (adds free electrons) could be Si in place of Ga since silicon has one more electron than gallium. The opposite kind of doping (p -type) would remove free electrons, potentially depopulating the valence band.

Control of the electrons and therefore the spin population can also be imposed by the use of a quantum heterostructure. These structures (typically nanoscale in size) are created by sandwiching the semiconductor between a material with a larger band gap (see Fig. 1.1). This creates a potential well that spatially restricts the electrons and thereby defines their excitation energies through quantization. Examples of these structures include wells, lines (wires), and dots which are confined in one, two, and three dimensions respectively. Such structures also tend to promote the formation of various quasi-particles, which can have a large effect on the spin dynamics of a sample.

1.1.3 Relevant Particles & Quasi-Particles

While this study focuses on the measurement of electron spin lifetimes, there are other particles present within our quantum well that greatly affect the dynamics of the spin population. These particles include holes, excitons, and trions.

A hole, strictly speaking, is not a particle, but rather the absence of one. A simple way to “create” one is to excite an electron from the valence band of a semiconductor to the conduction band (see Fig. 1.2). While the conduction band now has an extra electron, the valence band now has a “hole” where that electron used to be. In GaAs, holes are found in the three valence bands nearest the conduction band at the band gap ($\vec{k} = 0$): the heavy hole band, light hole band, and split-off band (see Fig. 1.2). The heavy and light labels refer to the effective masses of holes within these bands whereas the split-off band is so-called since it is separate from the others at $\vec{k} = 0$. In practice, usually only the heavy and light hole bands are considered relevant. The large energy gap between the split-off band and the heavy/light hole bands tends to force split-off holes to relax quickly to one of the other more energetically favorable bands (energetically favorable for a hole being the opposite of that for an electron). The distinction between heavy and light holes affects the spin dynamics of GaAs in two important ways. First, heavy and light holes have different spin due to a quantum effect known as spin-orbit coupling, whereby the normal electron spin of $1/2$ is combined with the orbital angular momentum value of 1 to form states of $\pm 3/2$ and $\pm 1/2$. Specifically, heavy holes are characterized by spin $\pm 3/2$ and light holes by $\pm 1/2$. Since the selection rules for optical excitation require the spin of the excited system to change by ± 1 , the different holes will respond differently under the same excitation. Second, a quantum well of GaAs lifts the degeneracy between the heavy and light hole bands normally present in GaAs, allowing one to tune to the optical transition of either hole.

Excitons and trions are not particles themselves but actually combinations of other particles that form a bound state. An exciton forms when an electron and a hole become bound by a Coulomb

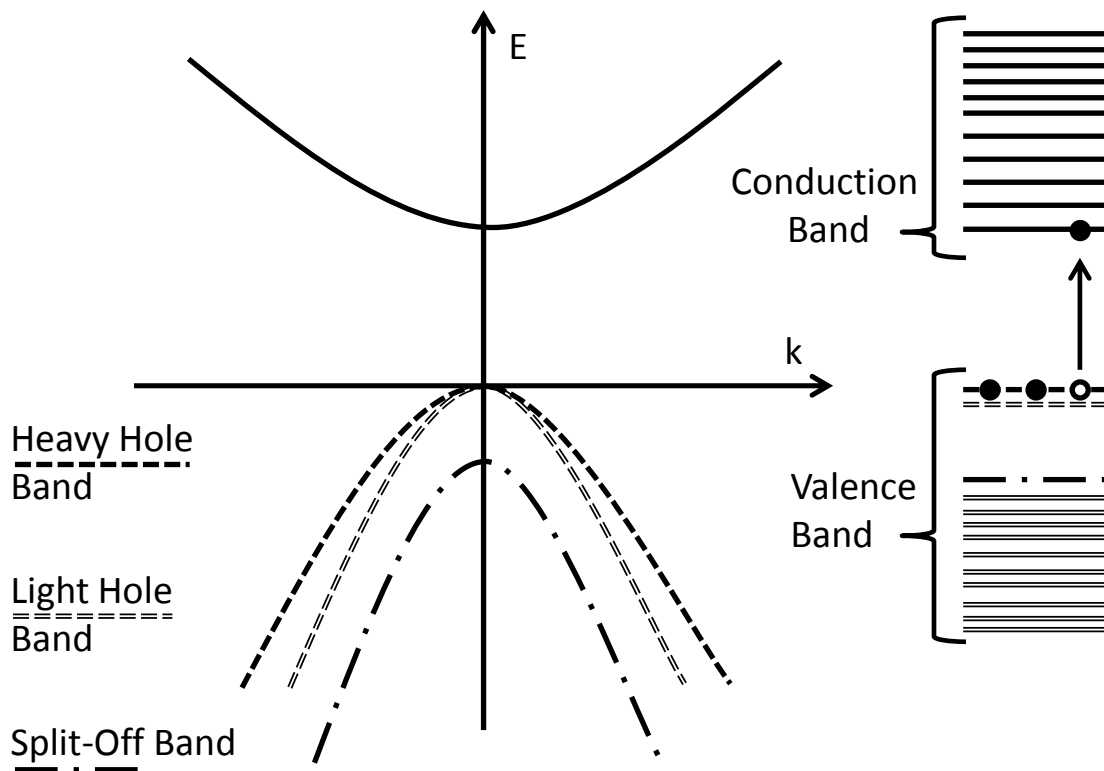


Figure 1.2 Approximate band structure of GaAs near $\vec{k} = 0$. Both the conduction and valence bands are formed by a near continuum of individual bands. The three bands of the valence band nearest the conduction band are the heavy hole band (dashed line), the light hole band (double dashed line), and the split-off band (dash-dot line). Electrons excited from the valence band leave empty space in the valence band that is called a “hole.” The type of hole depends on the band in which it is located.

interaction that produces a state of lower energy than a free electron and hole. There are two kinds of excitons, namely the light hole exciton and heavy hole exciton, which correspond to the type of hole that has formed the exciton. The most common method for forming an exciton is to excite an electron from the valence to the conduction band, forming a spatially close electron and hole. A trion, or charged exciton, is similarly formed using three instead of two particles. Typically, trions only form when doping is present and their charge mirrors that of the doping. In the case of n-type doping, negatively charged trions will form from two electrons and a hole. The ground state of this particular system is a singlet state where the spins of the electrons are anti-aligned, leaving the overall spin to correspond to the spin of the hole. Therefore, trions form in either light hole or heavy hole varieties with spin $\pm 1/2$ or $\pm 3/2$ respectively. How these particles and quasi-particles interact to form a spin population in our quantum well will be discussed in Section III of the included paper (pg. 12).

Chapter 2

Long-lived Electron Spins in a Modulation Doped (100) GaAs Quantum Well

The following paper, authored by my advisor, has been submitted for publication in the Journal of Applied Physics. My contributions as second author included taking measurements, analysis of acquired data, preparation of figures, literature research, and editorial assistance. It is presented here in its entirety, as submitted, in an effort to limit inadvertent plagiarism and to insure proper credit is given where due. It contains a detailed discussion of our results, how they were obtained, and an analysis of the various quantum mechanical mechanisms and interactions observed in our sample.

Long-lived electron spins in a modulation doped (100) GaAs quantum well

J. S. Colton, D. Meyer, K. Clark, D. Craft, J. Cutler, T. Park, P. White
Department of Physics and Astronomy, Brigham Young University, Provo UT

We have measured T_1 spin lifetimes of a 14 nm modulation-doped (100) GaAs quantum well using a time-resolved pump-probe Kerr rotation technique. The quantum well was selected by tuning the wavelength of the probe laser. T_1 lifetimes in excess of 1 microsecond were measured at 1.5 K and 5.5 T, exceeding the typical T_2^* lifetimes that have been measured in GaAs and II-VI quantum wells by orders of magnitude. We observed effects from nuclear polarization, which were largely removable by simultaneous nuclear magnetic resonance, along with two distinct lifetimes under some conditions that likely result from probing two differently-localized subsets of electrons.

PACS numbers: 72.25.Rb, 78.67.De, 78.47.jg, 72.25.Fe

I. INTRODUCTION

Since the initial proposal of spin-based quantum computing¹ and the discovery of very long inhomogeneous dephasing spin lifetimes (T_2^*) in GaAs,² a tremendous amount of research effort has been put forth to better understand the interaction of electronic spin states (“spins”) with each other and with their environment, and to create structures on the nanoscale that allow for better control and study of the spins.³ Among the key requirements for semiconductor spintronic devices is an understanding of the spin dephasing mechanisms in semiconductors.⁴ Optical techniques for interacting with spins in semiconductor heterostructures are powerful tools for the initialization, manipulation, and study of spin dynamics.⁵ GaAs/AlGaAs heterostructures are ideally suited for such experiments, as GaAs is a direct-gap semiconductor with well-known selection rules connecting optical polarization to the spin degree of freedom. Additionally, the band-gaps of GaAs/AlGaAs heterostructures readily match commercially-available lasers such as Ti:sapphire, which allows for resonant excitation and detection of the electronic spins.

Many experimental studies on GaAs have focused on lightly doped n -type bulk material, where electrons localize on donor sites at low temperature. Spin lifetimes much longer than the optical lifetimes can be obtained with these doped electrons. A wide variety of experimental techniques have been employed to study this type of bulk material, including (but not limited to) Hanle effect depolarization,⁶ time-resolved Faraday or Kerr rotation,^{2,7} optically-detected electron spin resonance,^{8,9} time-resolved decay of photoluminescence polarization^{10,11} or polarization-dependent luminescence,¹² optically-controlled spin echo,¹³ Kerr rotation imaging,^{14,15} and spin noise spectroscopy.¹⁶

Other experimental studies have focused on InAs or InGaAs quantum dots embedded in a GaAs barrier, again with doped electrons added to the dots to allow the electron spin information to be preserved beyond the radiative recombination time. In self-assembled quantum dots, for example, optical techniques have allowed the electron spins to be precisely controlled on time scales of micro- or milliseconds.¹⁷⁻²⁰

Bridging the gap between bulk material and 0D quantum dots, 2D systems can serve as well-defined model systems for studies in spin dynamics. Early studies of spins in quantum wells often focused on exciton dynamics.²¹ However, time-resolved studies have also served to shed light on properties of the electrons in GaAs quantum wells, allowing the dephasing of spins in subnanosecond²² and nanosecond^{23,24} time scales to be directly measured. The longest spin dephasing times in GaAs quantum wells have ranged from 10-30 ns.^{24,25} Other promising results have been obtained in II-VI quantum wells, where spin dephasing times of 30 ns have also been observed through various techniques^{26,27} and some degree of optical control of spins has been established.²⁸

Throughout these previous experiments, the spin lifetimes in quantum wells that have been the focus of research have nearly always been the T_2^* lifetimes, also called the inhomogeneous dephasing times. By contrast, in this paper we present experimental measurements of T_1 spin lifetimes, also known as spin flip times. While T_2^* is measured with the field perpendicular to the spin orientation, T_1 is measured with a parallel field. T_2^* and T_1 are generally considered lower and upper bounds for T_2 , the true dephasing time.

In this work we have measured the T_1 spin lifetime of a 14 nm GaAs quantum well using a time-resolved pump-probe Kerr rotation technique. The spin lifetimes were quite long—tens and hundreds of nanoseconds at most fields (from 0-7 T) and temperatures (1.5 and 5 K), and exceeding one microsecond at the lowest temperature and highest field. This paper is structured as follows: Sec. II describes the sample.

Sec. III discusses the polarization and detection scheme, along with some wavelength-dependent results. Sec. IV gives details on our experimental setup for spin lifetime measurements. The main experimental results and discussion are found in Sec. V, after which we provide some discussion in Sec. VI. We conclude in Sec. VII.

II. SAMPLE

We studied a 14 nm wide GaAs quantum well which was grown through molecular beam epitaxy and modulation doped with silicon donors to produce a carrier concentration of $n = 3 \times 10^{10} \text{ cm}^{-2}$ in the well. It is part of a multi-quantum well sample containing five total wells with thicknesses of 2.8, 4.2, 6.2, 8.4, and 14 nm. More details on the sample's structure and electronic properties can be found in Ref. 29. The 14 nm well was selected by tuning our laser to the optical transition of that well, approximately 807 nm. As with experiments in other n -type bulk, quantum dot, and quantum well samples mentioned in the Introduction, the doping allows spin information to be preserved through the ground state electrons.

This particular well of this particular sample has been the study of other spin-related investigations by our group and others, including Hanle effect measurements of T_2^* ,³⁰ time resolved Kerr rotation measurements to study optical initialization and T_2^* lifetimes,²³ and optically-detected electron spin resonance measurements which manipulated spin states with microwaves.³¹

III. SPIN POLARIZATION AND DETECTION

The modulation doping causes a background of electrons to exist in the well, which can interact with optically-injected excitons to form trion states. We consider only the lowest energy, singlet trions, where two electrons of opposite spin form a bound state with a hole which can be either spin-up or spin-down. The hole spin can be either $\pm 3/2$ or $\pm 1/2$, depending on whether it is a heavy or light hole. Because the two electrons in the singlet state have opposite spins, the overall spin of the trion follows the hole spin and is either $\pm 3/2$ or $\pm 1/2$. The details of trion formation rely critically on whether the optical photon has spin +1 (labeled σ^+) or spin -1 (labeled σ^-), and are depicted in Fig. 1.

The polarization of the ground state electron spins in doped quantum wells has typically been done through resonant excitation of a trion state.^{23,32,33} That mechanism relies on fast hole relaxation in the excited state: with σ^+ photons (for example) resonant with the heavy hole trion transition, electrons are taken out of the $+1/2$ state into the $+3/2$ heavy hole trion. The rapid hole relaxation causes the trion population to be equalized between the $+3/2$ and $-3/2$ states. In GaAs this can occur extremely

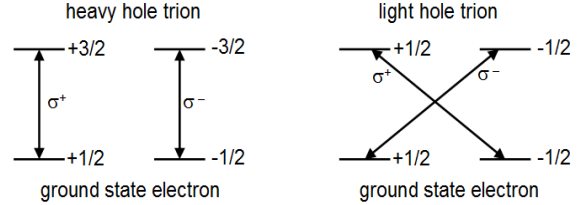


FIG. 1. Heavy and light hole trion transitions and selection rules. The trion forms when a ground state electron ($+1/2$ or $-1/2$) combines with an optically-injected electron hole pair. Because the two electrons are in a singlet state, the spin state of the trion matches the spin state of the hole ($+3/2$ or $-3/2$ for the heavy hole trion; $+1/2$ or $-1/2$ for the light hole trion). Photon spin states of $+1$ and -1 are indicated by σ^+ and σ^- respectively.

state, and a ground state spin polarization occurs. (If there were no hole spin flips, the $+3/2$ trion would simply decay back into the $+1/2$ ground state and no ground state spin polarization would accumulate.)

Our approach was slightly different. We performed a two-color experiment with pump and probe photons having different energies. Although our probe laser was resonant with a trion transition (details below), our pump laser (781 nm) was at a much higher energy. Our pump laser therefore excited both heavy and light hole trions simultaneously. Again considering σ^+ photons: they will excite heavy hole trions and pump spins out of the $+1/2$ ground state as described in the previous paragraph; however, they will also pump spins out of the $-1/2$ ground state by exciting light hole trions. As in the case of n -type bulk material—where the heavy and light hole states are degenerate at the band edge and are thus always excited simultaneously with a pump laser—we rely on unequal transition probabilities for the heavy hole state compared to the light hole state to generate a net spin polarization for the ground state electrons. Two-color experiments have been done in II-VI quantum wells in order to separate the effects of detecting the exciton vs. trion transitions,^{27,33,34} and have been proposed for use in a non-resonant pumping scheme such as we employed,³⁴ but we are not familiar with any other actual two-color experiments in GaAs quantum wells.

To detect the persisting electron spin polarization we tune the probe laser to be resonant with the trion transitions. This is quite similar to those groups cited above who employed a single-color resonant pump-probe scheme. We use the Kerr effect, i.e. the rotation of the angle of polarization of our linearly polarized probe beam, to detect the ground state spin population. Under typical conditions when the probe laser is tuned resonant with the quantum well's optical transition there is a clear signal with two features; see Fig. 2. The feature at 807.3 nm is from the light hole trion; the one at 808.1 nm is from the heavy hole trion. (As noted by Kennedy et al., the heavy hole *exciton* transition likely partially overlaps the light hole trion.²³) The peaks are opposite in sign because of the opposite selection rules depicted in Fig. 1.

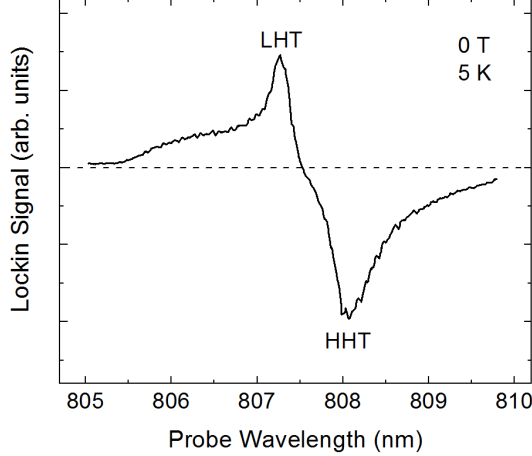


FIG. 2. Kerr rotation signal taken at 0 T, 5 K, as a function of probe laser wavelength. Data was obtained with pump and probe pulses each set for 50% duty cycle and overlapping each other in time. The dashed line indicates the zero position; the two peaks have opposite sign due to the optical selection rules. LHT and HHT label the light and heavy hole trion peaks, respectively.

In principle, the ground state electron spin polarization should be able to be measured through either the heavy hole or light hole trion transitions; in practice it proved easier for us to set our probe laser to the light hole trion transition because at some fields the heavy hole trion feature was difficult to observe; see Fig. 3a for a collection of wavelength-dependent data at various fields. The peak positions of Fig. 3a are summarized in Fig. 3b. The peak positions of the heavy and light hole trions as a function of magnetic field follow the well-known quadratic “diamagnetic shift,” in this case given by the following equations fitted from the data with energies in eV and fields in T:

$$E_{LHT} = 1.5360 + 4.289 \times 10^{-5} B^2 \quad (1a)$$

$$E_{HHT} = 1.5344 + 4.289 \times 10^{-5} B^2 \quad (1b)$$

The two trion peaks maintain a constant separation of 1.57 meV which is in good agreement for the LHT-HHT separation reported in Ref. 23.

IV. EXPERIMENTAL SETUP

To study the T_1 behavior of the ground state electron spins, we used a two-color pump-probe technique described in detail in Ref. 7. The magnetic field is oriented in Faraday (longitudinal) geometry, with the field parallel to the spin alignment. As mentioned in Section III, the spins are aligned using a circularly polarized pump laser and detected via the Kerr rotation of a linearly polarized probe laser. Both pump and probe lasers are pulsed, and the delay between the two of them is varied. This is similar to the traditional time resolved

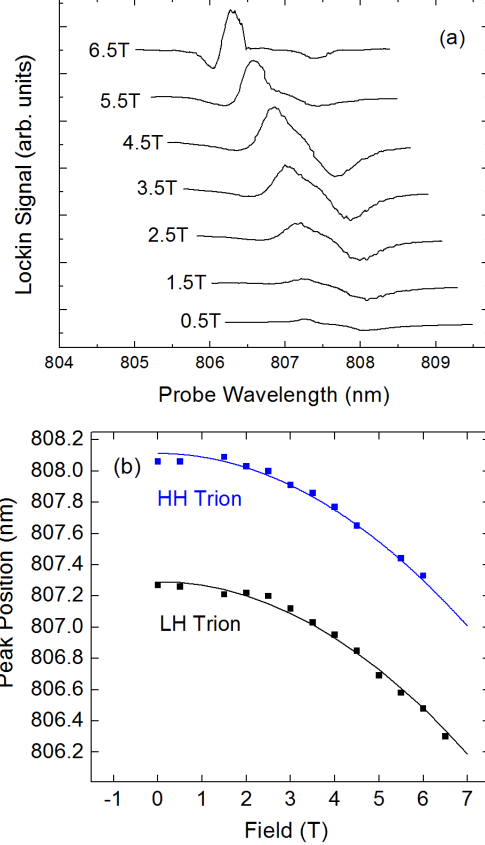


FIG. 3. (a) cw Kerr rotation signal vs. probe laser wavelength at 5 K for selected fields. Data was obtained under the same conditions as Fig. 2. (b) Summary of peak positions, fitted to a quadratic function in energy.

Kerr (or Faraday) rotation (TRFR) technique used by many to measure the inhomogeneous dephasing lifetime, T_2^* , of various semiconductors. However, in order to access the much longer lifetimes that are involved with T_1 as opposed to T_2^* , we employed electronic gating of pump and probe pulses instead of a mechanical delay line to vary the delay. Also, because the spins are parallel to the external field, we do not see the precession oscillations that are a hallmark of the traditional TRFR technique.

The pulses in the probe beam, a tunable cw Ti:sapphire laser, were produced with an acousto-optic modulator (AOM). Because the probe beam was quasi-cw—only pulsing on the time scales of tens of nanoseconds in response to our AOM—its bandwidth is essentially infinitely narrow on the scales of Figs. 2 and 3 and excellent wavelength resolution was achieved. The pump beam, a fast diode laser, was modulated on/off via a direct modulation input. The two beams were synchronously controlled with a two-channel pulse generator. To separate out the spin effects from sources of noise and to reduce dynamic nuclear polarization, we modulated the helicity of the pump laser from σ^+ to σ^- with a 42 kHz photoelastic modulator and detected the signal with a lockin amplifier referenced to that frequency. The lockin signal is proportional to the spin polarization of the electrons in

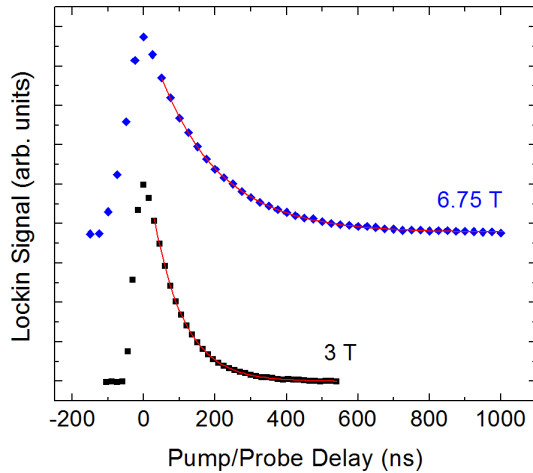


FIG. 4. Representative 5 K data taken at 3 T and 6.75 T: spin polarization vs. delay between pump and probe pulses. The raw data for the spin decays (points) was fitted to exponential decays (solid curves), yielding spin lifetimes of 84.5 ns and 169 ns for the 3 T and 6.75 T data, respectively. The 6.75 T data has been shifted vertically for clarity.

the sample.

The pump beam was set to 25 mW unpulsed and was focused (partially) to a diameter of 0.22 mm. The probe beam was set to a diameter of 0.21 mm and its power was either 3.5 mW unpulsed (for the 5 K data) or 2 mW unpulsed (for the 1.5 K data). The overall time for a pulse repetition cycle was approximately six times the decay time, and pulse widths were set to give the pump a duty cycle of 4% and the probe a duty cycle of 2%.

The sample was placed in a superconducting electromagnet with integrated cryostat where fields up to 7 T and temperatures down to 1.5 K could be investigated.

V. RESULTS

For a given set of experimental parameters, the delay between pump and probe was varied in order to trace out the decay of spin polarization. As the delay is varied, the probe pulse temporally “enters” the pump pulse, causing the lock-in signal to rapidly rise, then “exits” the pump pulse causing a decrease in signal. Any signal which exists after the probe pulse has exited the pump pulse is a result of persisting spin information. The polarization typically decays exponentially as:

$$P = P_0 \exp(-t/T_1) \quad (2)$$

See Fig. 4 for two representative decays and their fits, which in this case yielded spin lifetimes of 84.5 ns and 169 ns for the 3 T and 6.75 T data, respectively.

Figure 5 displays a summary of our spin lifetime results for spin decays measured at both 5 K and 1.5 K.

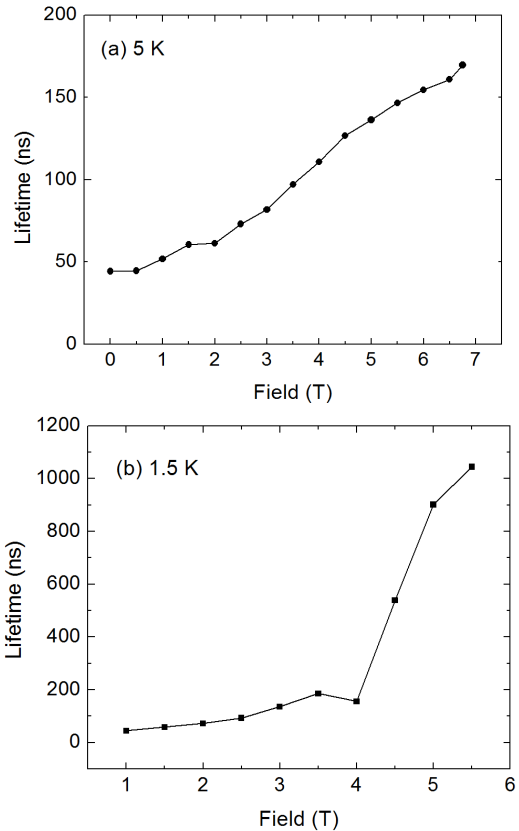


FIG. 5. Measured electron spin lifetimes as a function of magnetic field for (a) 5 K and (b) 1.5 K. For the 1.5 K data, the scans for fields at 4 T and above were done with rf applied to remove nuclear polarization (which may have caused some heating of the sample).

Spin lifetimes from 44 ns to 170 ns were measured at 5 K, and lifetimes from 44 ns to 1040 ns were measured at 1.5 K. These lifetimes far exceed the T_2^* value of 2.5 ns reported by Kennedy et al. for this particular quantum well (at 0 T, 6 K),²³ and are also much longer than the longest lifetimes (also T_2^*) of ~30 ns reported for *any* quantum wells of which we are aware, as referenced in the Introduction. T_1 is generally considered an upper bound for the true coherence time T_2 , and in (100) quantum wells T_2 is expected to be on the same order of magnitude as T_1 .⁴¹ Therefore these long T_1 results may be an indication that spin coherence can persist in quantum wells much longer than has generally been considered to be the case, and that e.g. spin echo experiments should be pursued in quantum well samples.

Nearly all of the raw data followed precise exponential decays like the two representative plots in Fig. 4. However, at 1.5 K there were some field points which did not follow a simple exponential decay. For those points, the lifetime that is plotted is simply the $1/e$ fall-off point for the raw data after the peak.

One reason for non-exponential decays is the presence of a nuclear spin polarization. Nuclear polarization is expected to arise whenever the electron spin polarization is far from thermal equilibrium. This is especially the case for us for the

high field, low temperature situations. From simple Boltzmann statistics, the polarization of a two level spin system is:

$$P = \tanh(g\mu_B B / 2k_B T) \quad (3)$$

The g -factor for this well was obtained in previous spin resonance experiments,³¹ $|g| = 0.346$, so at 1.5 K the thermal equilibrium polarization of the electrons will be 30%, 37%, and 43%, for fields of 4, 5, and 6 T, respectively. However, the pump laser—with its helicity modulated between σ^+ and σ^- as described above—will be driving the electron polarization towards 0%, at least on time scales long compared to the modulation time of $(42 \text{ kHz})^{-1}$. As the electrons are driven toward zero polarization, they will attempt to return to their thermal equilibrium value by interacting with the nuclear spin bath via the hyperfine interaction. This will polarize the nuclear spins to some degree. Polarized nuclei impact the electrons via the Overhauser effect and generate an effective field for the electrons. This effective field can vary both physically across our laser beams, as well as temporally during our scans, and can change the measured spin response in unpredictable ways.

That there *is* substantial nuclear spin polarization present in the material under some conditions was evident. Fig. 6 displays two spin decays taken at 5.5 T and 1.5 K, under nearly identical conditions. The only difference is that the solid curve was performed while rf was applied to a Helmholtz coil surrounding the sample, sweeping through the frequencies needed for nuclear magnetic resonance (NMR) of the four nuclear isotopes present in the quantum well and barrier: ^{75}As , ^{69}Ga , ^{71}Ga , and ^{27}Al . This was done via a function generator with customizable frequency modulation. With rf applied to remove built-up nuclear polarization, a relatively normal decay was observed. However, without rf the shape was both non-exponential and non-reproducible. As can be seen, for the data presented in Fig. 6 the spin polarization initially remained *constant* as the probe pulse begins to arrive after the pump. Something is changing inside the sample (i.e., the nuclear spins) in order to preserve the electron spin polarization! This is very reminiscent of the “spin dragging” effect that has been observed in electron spin resonance of bulk GaAs³⁵ and GaAs-based quantum dots,³⁶ where nuclear polarization has also been seen to adjust to keep the electronic polarization constant. These nuclear polarization effects were seen for all of the 1.5 K data at fields of 4 T and higher. The lifetimes plotted in Fig. 5b for these fields are for the “rf on” set of measurements. Although the decays for these points looked reasonable, as in the rf on curve of Fig. 5b, they could not be fitted to simple exponential decays—indicating that our removal of the effects from nuclear polarization was incomplete. The rf likely also caused some small heating of the sample, which could explain

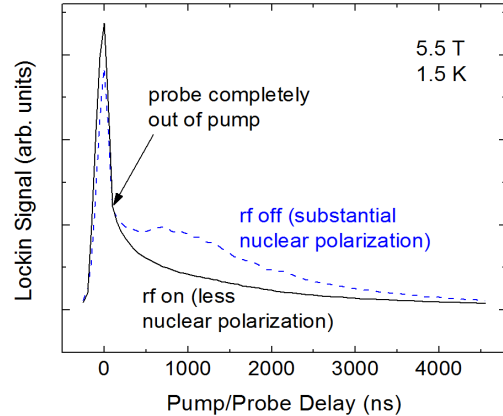


FIG. 6. Spin decays measured at 5.5 T and 1.5 K. The solid and dashed lines are for conditions with and without rf applied to depolarize the nuclear spins.

the unexpected decrease in lifetime in Fig. 5b going from 3.5 T (no rf) to 4 T (with rf).

VI. DISCUSSION

To discuss our spin relaxation results further, we first review some of the theoretical work on spin lifetimes in quantum wells. Spin scattering in quantum wells was first discussed by D'yakonov and Kachorovskii (DK).³⁷ In GaAs-based quantum wells, the lack of bulk inversion symmetry leads to spin-splitting of the conduction band. This spin splitting can be regarded as an internal magnetic field, about which electrons precess between momentum scattering events. This leads to information loss about the initial spin state and is called the D'yakonov-Perel mechanism. D'yakonov and Kachorovskii analyzed that mechanism in the context of quantum wells to obtain this result for the spin lifetime:

$$\tau_s = \frac{E_g \hbar^2}{\alpha^2 E_1^2 k_B T} \frac{1}{\tau_v}, \quad (4)$$

where E_g is the band gap energy, E_1 is the electron's quantized energy in the well, T is the temperature, τ_v is the momentum scattering time (which also depends on temperature), and α is a parameter related to the spin splitting of the conduction band. An important result is that generally speaking a short momentum scattering time (τ_v) will result in a long spin lifetime (τ_s), and vice versa. In asymmetric quantum wells, there is additionally a structural inversion asymmetry, which can add to or subtract from the effects of the bulk inversion asymmetry. This has recently been used in an experiment by Balocchi et al. to partially cancel the relaxation term from bulk inversion asymmetry (Dresselhaus) with the term from structural inversion asymmetry (Rashba).²⁴

The general theoretical approach is therefore often to model the momentum-scattering mechanisms that contribute to τ_s ; for example, Bastard and Ferreira used the DK theory to describe

ionized impurity scattering, often the most efficient scatterers at low T.³⁸ They found that τ_s shortens considerably at low temperatures due to inefficient screening, yielding spin flip times that are the longest for wide wells and low temperatures. For their particular impurity concentration and screening model, they predicted τ_s to be 2.5 ns at 10 K for a 15 nm GaAs/AlGaAs well and their data points suggest that τ_s should increase rapidly with a decreasing temperature. A simple extrapolation of their data suggests a factor of 10 or 100 increase in lifetime as temperature decreases to 1.5 K. Bastard extended the DK theory to a high magnetic field situation using Landau levels and a point-like defect model for the scatterers, to obtain a prediction of 1-2 ns for a 9 nm well for fields between 6 and 15 T and a $B^{1/2}$ dependence of lifetime on field.³⁹

Experimentally, Terauchi et al. measured spin lifetimes at 0 T and 300 K in a series of 7.5 nm multi-quantum well samples, and verified the $\tau_s \sim 1/\tau_v$ prediction of the DK theory, although the spin lifetimes were about an order of magnitude higher than the theory predicted.⁴⁰ Lau et al. built upon the DK theory in two papers, using a 14 band $\mathbf{k}\cdot\mathbf{p}$ model to describe bulk⁴¹ and structural inversion asymmetry,⁴² and overcame the order of magnitude discrepancy that had been seen. T_1 and T_2 were predicted to be the same order of magnitude, with T_2 ranging from $2T_1/3$ to $2T_1$ in (100) wells depending on the value of α . Their calculated T_1 values matched the room temperature experiments of Terauchi et al.,⁴⁰ and the T_2 values matched the original experiments of Kikkawa and Awschalom² for temperatures of 100 K and above. They issued the disclaimer, however, that their theory might not be applicable at lower temperatures.

More recent theory on spin relaxation in n -doped quantum wells is sparse, the work of Harmon et al. being a notable exception.⁴³ Their work focuses on spin dephasing from the hyperfine interaction, applicable to T_2^* but not to T_1 . They also explicitly account for doping via donors inside the well, and mention that their theory is consequently not applicable for modulation doped wells (such as used in our experiment).

Considering our measured value of 44 ns for T_1 at 0 T and 5 K, our results seem fairly solidly in the Bastard and Ferreira regime (if the low temperature extrapolation of their data is to be believed), and likely indicates that ionized impurity scattering within the DK model is our primary relaxation mechanism. Our quantum well is modulation doped, so there are no *intentional* impurities in the well, but this sample did have a slight n -type background. Our spin lifetime increase with magnetic field did not exactly follow the $B^{1/2}$ prediction of Bastard, but our lifetimes did increase nearly monotonically with field as Bastard's theory predicts. Comparing our results to other experimental results, one would expect our 0 T, 5 K value for T_1 to match fairly closely the 0 T, 6 K value for T_2^* of Kennedy et al.,²³ since the sample is the same and T_2^* and T_1 are equivalent in the absence of a

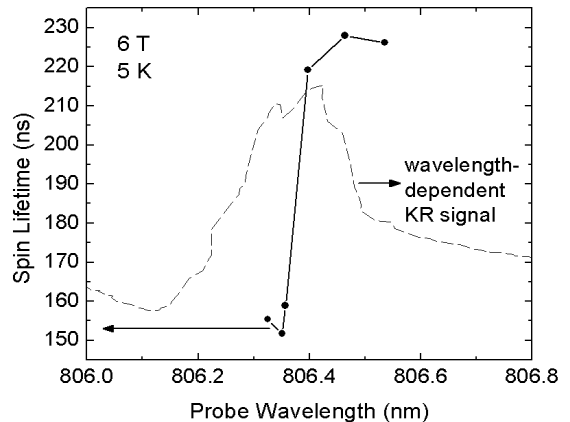


FIG. 7. Spin lifetimes as a function of probe laser wavelength, for 6 T and 5 K. Note the abrupt shift in lifetime over a very small wavelength range. For reference, the wavelength-dependent Kerr rotation for these conditions, showing the light hole trion peak, is also displayed (dashed).

magnetic field. However, the value of Kennedy et al. seems to have been obtained from a fit of a decay measured only between 0 and 1.5 ns, and consequently their value of 2.5 ns may not be completely trustworthy.

Finally, in two previous papers on T_2^* lifetimes in II-VI quantum wells, two distinct spin lifetimes were seen for a given temperature and field.^{27,34} In each case the difference arose when detecting the spin of the electrons through the trion transition vs. through the exciton transition: a factor of 6 difference in lifetime for Ref. 27 and a factor of 2 for Ref. 34. Each group attributed the difference in lifetimes to a difference in localization of the subset of electrons being probed: localized electrons in the case of the trion transition and quasi-free electrons in the case of the exciton transition. The trion and exciton transitions are clearly resolvable in II-VI quantum wells, but in our GaAs quantum well the light hole trion transition and heavy hole exciton were likely both contained in the “light hole trion region” marked on Fig. 2 (which is where we probed). Nevertheless, we may have seen this effect in our T_1 measurements as well. Fig. 7 displays the results of a fine-scale wavelength adjustment: measuring the spin lifetimes as we varied the probe laser across the light hole trion peak. The trion peak from the non-time-resolved wavelength-dependent Kerr rotation signal is shown dashed. As the wavelength was tuned from one side of the peak to the other, there was an abrupt shift in spin lifetime. It seems likely that this shift in lifetime is a result of probing different subsets of electrons (e.g. localized vs. quasi-free) electrons, just as was seen in the II-VI quantum well experiments.

VII. CONCLUSION

In conclusion, we have measured T_1 spin flip times in a GaAs quantum well by tuning a probe laser to be resonant with the optical transition of the well in a longitudinal (Faraday) geometry. The well had extremely long spin

lifetimes, exceeding one microsecond for 1.5 K and 5.5 T. This quite likely indicates long T_2 lifetimes as well. Lifetimes increase with field, and decrease with temperature. Nuclear polarization effects were significant at the highest fields at 1.5 K, but could largely

be removed with nuclear magnetic resonance. Different lifetimes were observed with small changes in wavelength for one set of experimental conditions, likely indicating responses from two differently-localized subsets of electrons.

- ¹ D. Loss and D. P. DiVincenzo, Phys. Rev. A **57**, 120 (1998).
- ² J. M. Kikkawa and D. D. Awschalom, Phys. Rev. Lett. **80**, 4313 (1998).
- ³ See M. W. Wu, J. H. Jiang, and M. Q. Weng, Phys. Rep. **493**, 61 (2010) for a recent and extensive review article on the topic.
- ⁴ *Spin Physics in Semiconductors*, edited by M. I. Dyakonov (Springer, Berlin, 2008).
- ⁵ *Optical Orientation*, edited by F. Meier and B. P. Zakharchenya (North-Holland, Amsterdam, 1984).
- ⁶ R. I. Dzhioev, K. V. Kavokin, V. L. Korenev, M. V. Lazarev, B. Ya. Meltser, M. N. Stepanova, B. P. Zakharchenya, D. Gammon, and D. S. Katzer, Phys. Rev. B **66**, 245204 (2002).
- ⁷ J. S. Colton, K. Clark, D. Meyer, T. Park, D. Smith, and S. Thalman, Solid State Comm. **152**, 410 (2012).
- ⁸ J.S. Colton, T.A. Kennedy, A.S. Bracker, D. Gammon, and J.B. Miller, Phys. Rev. B **67**, 165315 (2003).
- ⁹ J.S. Colton, T.A. Kennedy, A.S. Bracker, D. Gammon, and J. Miller, Solid State Comm. **132**, 613 (2004).
- ¹⁰ J. S. Colton, T. A. Kennedy, A. S. Bracker, and D. Gammon, Phys. Rev. B **69**, 121307(R) (2004).
- ¹¹ J. S. Colton, M. E. Heeb, P. Schroeder, A. Stokes, L. R. Wienkes, and A. S. Bracker, Phys. Rev. B **75**, 205201 (2007).
- ¹² K.-M. Fu, W. Yeo, S. Clark, C. Santori, C. Stanley, M. C. Holland, and Y. Yamamoto, Phys. Rev. B **74**, 121304(R) (2006).
- ¹³ S. M. Clark, K.-M. Fu, Q. Zhang, T. D. Ladd, C. Stanley, and Y. Yamamoto, Phys. Rev. Lett. **102**, 247601 (2009).
- ¹⁴ J. Kikkawa, D. Awschalom, Nature **397**, 139 (1999).
- ¹⁵ S. A. Crooker and D. L. Smith, Phys. Rev. Lett. **94**, 236601 (2005).
- ¹⁶ S. A. Crooker, L. Cheng, and D. L. Smith, Phys. Rev. B **79**, 035208 (2009).
- ¹⁷ M. Kroutvar, Y. Ducommun, D. Heiss, M. Bichler, D. Schuh, G. Abstreiter, and J. F. Finley, Nature **432**, 81 (2004).
- ¹⁸ A. Greilich, D. R. Yakovlev, A. Shabaev, Al. L. Efros, I. A. Yugova, R. Oulton, V. Stavarache, D. Reuter, A. Wieck, and M. Bayer, Science **313**, 341 (2006).
- ¹⁹ A. Greilich, A. Shabaev, D. R. Yakovlev, Al. L. Efros, I. A. Yugova, D. Reuter, A. D. Wieck, and M. Bayer, Science **317**, 1896 (2007).
- ²⁰ D. Press, K. De Greve, P. L. McMahon, T. D. Ladd, B. Friess, C. Schneider, M. Jamp, S. Höfling, A. Forchel, and Y. Yamamoto, Nature Photon. **4**, 367 (2010).
- ²¹ See Chapter 3 of Reference 4 for a review: T. Amand and X. Marie, *Exciton Spin Dynamics in Semiconductor Quantum Wells*.
- ²² A. Malinowski and R. T. Harley, Phys. Rev. B **62**, 2051 (2000).
- ²³ T. A. Kennedy, A. Shabaev, M. Scheibner, A. L. Efros, A. S. Bracker, and D. Gammon, Phys. Rev. B **73**, 045307 (2006).
- ²⁴ A. Balocchi, Q. H. Duong, P. Renucci, B. L. Liu, C. Fontaine, T. Amand, D. Lagarde, and X. Marie, Phys. Rev. Lett. **107**, 136604 (2011).
- ²⁵ R.I. Dzhioev, V.L. Korenev, B.P. Zakharchenya, D. Gammon, A.S. Bracker, J.G. Tischler, D.S. Katzer, Phys. Rev. B **66**, 153409 (2002)
- ²⁶ E.A. Zhukov, D.R. Yakovlev, M. Bayer, G. Karczewski, T. Wojtowicz, J. Kossut, Phys. Stat. Sol. (b) **243**, 878 (2006)
- ²⁷ H. Hoffmann, G.V. Astakhov, T. Kiessling, W. Ossau, G. Karczewski, T. Wojtowicz, J. Kossut, L.W. Molenkamp, Phys. Rev. B **74**, 073407 (2006)
- ²⁸ E. A. Zhukov, D. R. Yakovlev, M. M. Glazov, L. Fokina, G. Karczewski, T. Wojtowicz, J. Kossut, and M. Bayer, Phys. Rev. B **81**, 235320 (2010).
- ²⁹ J. G. Tischler, A. S. Bracker, D. Gammon, and D. Park, Phys. Rev. B **66**, 081310(R) (2002).
- ³⁰ R. I. Dzhioev, V. L. Korenev, I.A. Merkulov, B. P. Zakharchenya, D. Gammon, Al. L. Efros, and D. S. Katzer, Phys. Rev. Lett. **88**, 256801 (2002).
- ³¹ B. Heaton, J.S. Colton, D.N. Jenson, M.J. Johnson, and A.S. Bracker, Solid State Comm. **150**, 244 (2010).
- ³² W. Ungier and R. Buczko, J. Phys.: Condens. Matter **21**, 045802 (2009).
- ³³ Z. Chen, S. G. Carter, R. Bratschitsch, and S. T. Cundiff, Physica E **42**, 1803 (2010).
- ³⁴ E.A. Zhukov, D.R. Yakovlev, M. Bayer, M.M. Glazov, E.L. Ivchenko, G. Karczewski, T. Wojtowicz, and J. Kossut, Phys. Rev. B **76**, 205310 (2007).
- ³⁵ T. A. Kennedy, J. Whitaker, A. Shabaev, A. S. Bracker, and D. Gammon, Phys. Rev. B **74**, 161201R (2006).
- ³⁶ I. T. Vink, K. C. Nowack, F. H. L. Koppens, J. Danon, Y. V. Nazarov, and L. M. K. Vandersypen, "Locking electron spins into magnetic resonance by electron–nuclear feedback," Nat. Phys. **5**, 764 (2009).
- ³⁷ M. I. D'yakonov and V. Yu. Kachorovskii, Sov. Phys.-Semicond. **20**, 110 (1986).
- ³⁸ G. Bastard, R. Ferreira, Surf. Sci. **267**, 335 (1992).
- ³⁹ G. Bastard, Phys. Rev. B **46**, 4253 (1992).
- ⁴⁰ R. Terauchi, Y. Ohno, T. Adachi, A. Sato, F. Matsukura, A. Tackeuchi, and H. Ohno, Jpn. J. Appl. Phys. **38**, 2549 (1999).
- ⁴¹ W. H. Lau, J. T. Olesberg, and M. E. Flatte, Phys. Rev. B **64**, 161301 (2001).
- ⁴² W. H. Lau and M. E. Flatte, J. Appl. Phys. **91**, 8682 (2002).
- ⁴³ N. J. Harmon, W. O. Putikka, and R. Joynt, Phys. Rev. B **81**, 085320 (2010).

Chapter 3

Further Discussion

3.1 An Unexplained Effect

There is one final note to be made regarding our results, particularly the wavelength scans presented in Section III of the included paper. For the bulk of our wavelength scans, the sweep direction of the probe laser wavelength was inconsequential; sweeping either from short to long wavelength or vice-versa would produce the same result. However, this invariance with respect to sweep direction was not always present at higher magnetic fields. Under these conditions, we would sometimes find that sweep direction had a huge effect on our results (see Fig. 3.1a for an example). With all else held constant, we found that we could repeatedly scan up from short to long wavelength then back down from long to short wavelength and trace two distinct curves. This effect did not prove to be very reproducible from day-to-day, with either curve shapes changing or the effect being completely absent under the same conditions, but was perfectly reproducible on a time scale of tens of minutes.

We also found that with our probe laser tuned to a wavelength that would produce two widely different signals depending on sweep direction (like the large negative peak of Fig. 3.1a), we could

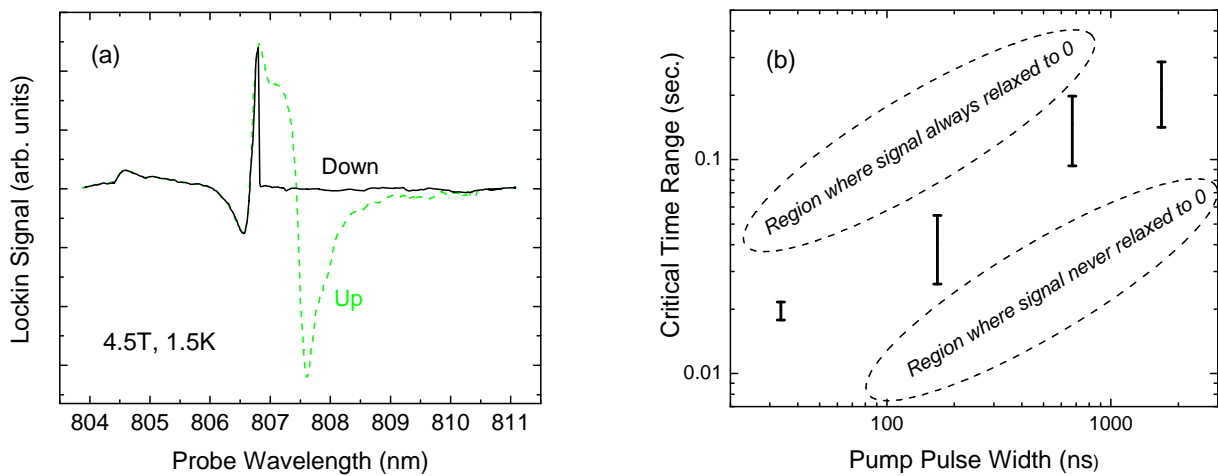


Figure 3.1 (a) Wavelength dependent cw Kerr rotation scans. Both curves were obtained under otherwise identical conditions (4.5 T, 1.5 K) by varying the wavelength from low to high (dashed curve) and from high to low (solid curve). (b) The critical pump beam blocking times for different pump pulse widths at 4 T, 1.5 K, plotted using a Log-Log scale. With the probe wavelength set to a condition where two different signals were obtained dependent on sweep direction, the pump beam was blocked for a short time. The length of time blocked relative to the critical range of times governed the signal response.

induce transitions from the larger signal to the smaller by blocking the pump beam for a short period of time. Interestingly, if the beam was blocked for too short a time, the transition would not occur. By using a fast photodiode with a digital timer under conditions nearly identical to Fig. 3.1a, we were able to identify a critical range of times for various pump beam pulse widths (see Fig. 3.1b). If the pump beam was blocked for a time longer than the critical range, the transition would always occur. If the pump beam was blocked a shorter time, the transition would never occur. If the blocking time was within the critical range, whether the transition occurred or not was apparently random. The critical times ranged from ~ 20 to ~ 200 milliseconds as the pump pulse was varied from 30 to 1700 nanoseconds.

Unfortunately, the source of this effect is still a mystery. While the irreproducibility from day-to-day as well as the general behavior of the effect seem reminiscent of the nuclear polarization described in Section V of the included paper (pg. 14), it seems unlikely that nuclear polarization is to blame. Not only was the effect observed at 5 K, a relatively high temperature for nuclear polarization, but the application of resonant rf did not remove the effect. Especially considering that rf was very effective at improving our spin decays under similar conditions (see Fig. 6 of the included paper, pg. 15), nuclear polarization can likely be ruled out as the cause of this effect.

3.2 Conclusion

In summary, we have found that the 14nm GaAs/AlGaAs quantum well exhibits unique spin dynamics. Most importantly, T_1 spin flip times in excess of a microsecond under conditions of 1.5 K and 5.5 T were observed. Secondly, the data suggests that the different subsets of electrons corresponding to heavy and light hole trions can have different spin flip times under the same conditions. Nuclear polarization was observed given high magnetic field and low temperatures and responded to the application of resonant rf. Finally, sweeping the probe wavelength revealed that

signal response is dependent on sweep direction under certain conditions. Furthermore, a transition between the signal responses from the two sweep directions could be induced by blocking the pump beam. We were unable to identify the cause of these final two effects.

Bibliography

- [1] D. Loss and D. P. DiVincenzo, Phys. Rev. A **57**, 120 (1998).
- [2] J. M. Kikkawa and D. D. Awschalom, Phys. Rev. Lett. **80**, 4313 (1998).
- [3] M. S. A. L. E. A. S. B. T. A. Kennedy, A. Shabaev and D. Gammon, Phys. Rev. B **73**, 045307 (2006).

Index

- D'yakonov-Kachorovskii (DK) Theory, 15
- D'yakonov-Perel Mechanism, 15
- Doping, 3
- Electron Spin, 2
- Faraday (Longitudinal) Geometry, 3, 13
- Kerr Rotation, 12
- Nuclear Polarization, 14
- Particles, 5
 - Excitons, 5
 - Holes, 5
 - Trions, 7
- Quantum Heterostructures, 4
- Semiconductors, 3
- Spin Lifetimes, 2, 11
 - T_1 , Spin-Flip Time, 2
 - T_2 , Dephasing Time, 3
 - T_2^* , Inhomogeneous Dephasing Time, 3
- Time Resolved Faraday Rotation (TRFR), 13
- Voigt (Transverse) Geometry, 3